NO and NO_2 Adsorption on Terrace, Step, and Corner Sites of the BaO Surface from DFT Calculations

Maria Marta Branda,† Cristiana Di Valentin, and Gianfranco Pacchioni*

Dipartimento di Scienza dei Materiali, Università di Milano-Bicocca, and Istituto Nazionale per la Fisica della Materia, via R. Cozzi, 53 - I-20125 Milano, Italy

Received: June 30, 2003; In Final Form: January 26, 2004

The adsorption of NO and NO_2 molecules at the BaO surface has been investigated by means of density functional theory (DFT) cluster model calculations. Regular adsorption sites at flat terraces have been compared with those on steps and corners. The properties of the adsorbed molecules have been monitored by computing various observable properties, such as core level binding energies, hyperfine coupling constants, and vibrational frequencies. NO binds strongly at the oxide anions at terraces, steps, and corners of the BaO surface. The bonding has a substantial polarity due to delocalization of charge from the surface to the adsorbate, but cannot be described as a full charge transfer interaction. The spin is almost entirely localized on the NO adsorbed molecule. NO_2 binds to the BaO surface in two different ways, N-down and O-down. In both orientations the oxide anion on the surface is oxidized with formation of an NO_2^- species which interacts electrostatically with the neighboring Ba cations. The spin is localized on the surface anions by the effect of the creation of a hole in the O(2p) valence shell. The O-down mode is more stable on terrace sites, while on low-coordinated sites the two orientations have similar stabilities. For both NO and NO_2 the low-coordinated sites exhibit a much larger reactivity than the flat terraces. The formation of O^- ions in the case of NO_2 adsorption can be very important for the further reactivity of the surface.

1. Introduction

The interaction of NO_x with oxide surfaces turns out to be an important aspect in the catalytic conversion of car exhausts. Several investigations have been dedicated to the adsorption and reactivity of NO_x on alumina-supported BaO particles.[1,2] The reactions taking place are rather complex as they include competition of NO_x with CO_2 bonding, reaction with hydroxyl groups, various oxidation steps, etc. BaO is used as a storage catalyst which traps NO_2 and releases NO through conversion of surface nitrites to nitrates. So far, a lot of attention has been dedicated to the interaction of gas-phase NO_x species with the surface of a model system like MgO,[3,4] with fewer studies dedicated to heavier alkaline-earth oxides. From a theoretical point of view very few studies have been reported on the BaO surface.[5−9] In a periodic supercell density functional theory (DFT) study Broqvist et al.[7] have investigated, for the first time, the interaction of NO_2 with the surface of BaO, the subsequent reaction of the surface species, and the possible reaction paths that lead to the release of NO. Very recently, a comparative cluster model DFT study of NO_2 adsorption on the series of alkaline-earth-metal oxides has been reported by Pettersson et al.[8] In both these studies only flat (100) terrace sites have been considered, and the complexity due to the presence of surface defects has not been addressed.

Surface defects on other alkaline-earth oxides play a fundamental role in several processes. For a rather unreactive oxide like MgO they determine the entire reactivity of the system, the (100) faces being completely inert.[10] Things may be different when one goes from MgO to BaO. It is well-known that the surface basicity increases going down the series,[11,12] and a rationalization of the different reactivity of MgO versus CaO flat terraces has been provided in terms of the reduction of the Madelung potential in CaO due to the longer cation−anion distances.[13] This effect is expected to lead to a highly reactive BaO surface. However, this does not rule out the possibility that special reactions take place at defect sites such as steps or corners. Also, in this case it has been possible to rationalize the different behavior of these sites compared to the five-coordinated terrace sites on the basis of a reduced Madelung field.[13]

In this work we have studied the interaction of isolated NO and NO_2 molecules with the regular, step, and corner sites at the BaO surface using embedded cluster models. Thus, cooperative effects recently discovered in the adsorption of NO_2 on oxide surfaces have not been considered.[3] We have determined observable properties such as the binding energy, the vibrational frequency, the shifts in core level binding energies, and the hyperfine coupling constants. The results show that the BaO surface is much more reactive than the MgO one, and that low-coordinated sites are more active than the terrace sites. NO binds much more strongly on these low-coordinated sites than on the flat terraces, but the bonding mechanism is similar in the two cases. For NO_2 a full charge transfer occurs from the oxide anions of the surface to the molecules adsorbed at steps and corners, while only partial charge transfer occurs on the terrace sites. This shows that the study of chemical properties of the BaO surface must also include the analysis of the surface properties of the defect sites.

2. Computational Details

Density functional theory (DFT) quantum-mechanical calculations were carried out using the gradient-corrected Becke

* Corresponding author. E-mail: gianfranco.pacchioni@unimib.it.
† On leave from Departamento de Fisica, UNS, Av. Alem 1253 (8000) Bahia Blanca, Argentina.

10.1021/jp035862b CCC: $27.50
Published on Web 03/12/2004

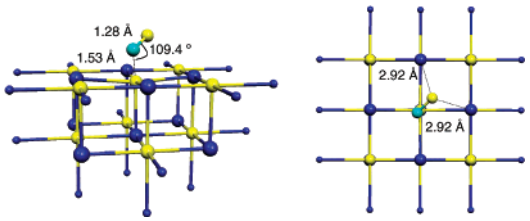

Figure 1. Optimal structure of an NO molecule adsorbed on an O_{5c} oxide anion at the terrace sites of the BaO surface (left, side view; right, top view). The surface is represented by a $Ba_9O_9Ba^*_{16}$ cluster embedded in point charges (not shown). Yellow spheres, O; sky-blue sphere, N; large blue spheres, Ba; small blue spheres, Ba*.

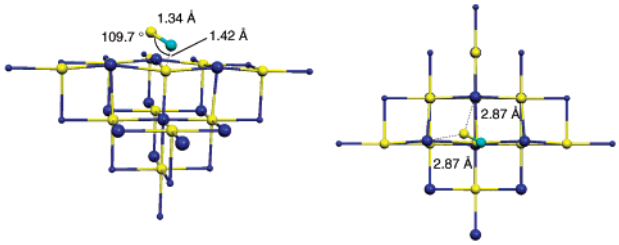

Figure 2. Optimal structure of an NO molecule adsorbed on an O_{4c} oxide anion at the step sites of the BaO surface (left, side view; right, top view). The surface is represented by a $Ba_{11}O_{11}Ba^*_{13}$ cluster embedded in point charges (not shown). Yellow spheres, O; sky-blue sphere, N; large blue spheres, Ba; small blue spheres, Ba*.

three-parameter hybrid exchange functional[14] in combination with the correlation functional of Lee, Yang, and Parr[15] (B3LYP).

To calculate the properties of NO and NO_2 molecules adsorbed on the BaO surface, we employed an embedded cluster model approach. The BaO(100) surface is represented by finite BaO stoichiometric clusters embedded in ±2 point charges (PCs). In doing this a full ionic model has been assumed. Accurate analyses of the bonding show that the degree of ionicity in alkaline-earth oxides with NaCl structure decreases going from MgO to BaO but that even BaO has about 90% ionic character.[16] The large array of PCs is aimed at reproducing the Madelung potential at the adsorption site. To avoid the artificial polarization of the O^{2-} anions at the cluster border induced by the PCs,[17,18] we have replaced the positive PCs at the interface by effective core potentials (ECPs)[19] which provide a representation of the finite size of the Ba^{2+} cation. The interface Ba cations treated in this way are denoted in the following as Ba*. No basis functions are associated with these atoms. This approach has been used in the past in the study of other ionic oxides such as MgO and has been compared to periodic approaches and more elaborate embedding schemes based on Green's functions.[20]

Various BaO adsorption sites have been considered: regular (100) terraces, O_{5c}, four-coordinated anions at steps, O_{4c}, and three-coordinated anions at corners, O_{3c}. The clusters used are $Ba_9O_9Ba^*_{16}$ for terrace, $Ba_{11}O_{11}Ba^*_{13}$ for step, and $Ba_{10}O_{10}$-Ba^*_{12} for corner; see Figures 1−3. A Ba−O distance of 2.76 Å has been used to construct the clusters. The O atoms have been described with a 6-31+G* basis set. The Ba atoms have been treated with a small core ECP which includes in the valence the $5s^25p^66s^2$ electrons; the Ba basis set is that originally derived by Hay and Wadt[21] with the contraction scheme implemented in the Gaussian98 code[22] (LANL2DZ)[23] and augmented by one d polarization function directly optimized on the Ba_9O_9 cluster ($\alpha_d = 0.275$). The addition of one d polarization function is important since it has been shown that the 5d states contribute

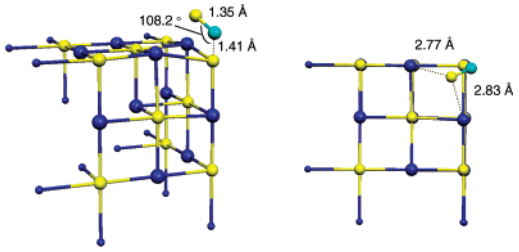

Figure 3. Optimal structure of an NO molecule adsorbed on an O_{3c} oxide anion at the corner sites of the BaO surface (left, side view; right, top view). The surface is represented by a $Ba_{10}O_{10}Ba^*_{12}$ cluster embedded in point charges (not shown). Yellow spheres, O; sky-blue sphere, N; large blue spheres, Ba; small blue spheres, Ba*.

to the bonding with the oxide anions in the bulk.[24] The NO and NO_2 molecules have been treated at the all-electron level using the 6-31+G* basis set. The interaction energies have been corrected by the basis set superposition error (BSSE) using the counterpoise correction.[25]

Geometry optimizations have been performed by means of analytical gradients with no symmetry constraints. For adsorption on the terrace sites the adsorbed NO or NO_2 molecules and either the central oxide anion or the two central barium cations, according to the adsorption mode, were free to relax; on the step and the corner sites, beside the central oxygen anion, also the four and the three Ba neighbors, respectively, have been included in the geometry optimization.

Vibrational frequencies have been computed by determining the second derivatives of the total energy with respect to the internal coordinates. With the present approach the N−O stretching frequencies computed for the free NO and NO_2 molecules are overestimated with respect to experiment by about 5%. Thus, a scaling factor 0.95 has been applied to all the computed frequencies. The vibrational frequencies have been determined only for the terrace sites since these are the majority of the surface sites.

We have determined the core level binding energies of the O(1s) and N(1s) levels of the adsorbed NO and NO_2 molecules and of the oxide anion where they are bound. The core level shifts with respect to the separate noninteracting units, BaO and NO or NO_2, or the corresponding anions, NO^- or NO_2^-, provide a qualitative, not a quantitative, measure of the charge transfer from the surface to the adsorbate since several effects contribute to the final shift.[26−28] We used changes of the Kohn−Sham eigenvalues, $-\epsilon_i$, as a measure of the shifts in core level binding energies occurring upon adsorption.

NO and NO_2 are paramagnetic molecules. Their spin properties on the BaO surface are accessible to electron paramagnetic resonance, EPR. The hyperfine interaction of the electron spin with the nuclear spin of the ^{17}O and ^{14}N nuclides has been determined. The hyperfine spin-Hamiltonian, $\mathbf{H}_{hfc} = \mathbf{S}\cdot\mathbf{A}\cdot\mathbf{I}$, is given in terms of the hyperfine matrix **A**, which describes the coupling between the electronic and the nuclear spins.[29] The components of **A** can be represented as the sum of an isotropic part, a_{iso}, related to the Fermi contact term, and the matrix **B**, which represents the "classical" dipolar interaction between two magnetic (electronic and nuclear) moments. Typical anisotropic interactions can be observed when the unpaired electron is in directional orbitals such as p, d, f, etc. The **A** tensor can therefore be represented in matrix notation as $\mathbf{A} = a_{iso} + \mathbf{B}$.

The calculations have been performed using the Gaussian98 program package.[22]

3. Results and Discussion

3.1. The BaO Surface. The description of the reactivity of the BaO surface depends critically on the reproduction of some key properties, such as the energy gap and the position of the top of the O(2p) valence band. Cluster models are inadequate to properly reproduce these quantities, but one can use the corresponding HOMO−LUMO energy gap as a crude measure of the band gap of the material or the vertical ionization potential (IP) as an indication of the position of the top of the valence band with respect to the vacuum level. With the $Ba_9O_9Ba^*_{16}$ model of the regular (100) surface the HOMO−LUMO gap is 2.84 eV. The band gap in the bulk oxide is 3.8 eV.[30,31] Usually the gap on the surface is reduced compared to the bulk; in MgO the gap for the (100) surface, 6.8 eV, is about 1 eV smaller than for the bulk, 7.8 eV.[32] Assuming a similar reduction for BaO, the computed value of 2.8 eV seems quite realistic. The vertical IP for the same cluster is 4.09 eV; the hole created in the ionization process is delocalized over the oxygen atoms of the cluster. This suggests that the top of the O(2p) valence band is positioned about 4.1 eV below the vacuum level. However, some uncertainty in the calculation of this value is due to the absence of long-range polarization effects which stabilize the ionized state, thus reducing the value of the IP. For comparison, the position of the top of the valence band in MgO is about 6.7 eV below the vacuum level.[32] The fact that the top of the valence band in BaO is more than 2 eV higher than in MgO is consistent with the smaller Madelung potential in the heavier oxide and has important consequences for the explanation of the different reactivity of the two surfaces. Of course, lower IPs are found for the low-coordinated sites: 3.42 eV for a step and 3.69 eV for a corner. Thus, an enhanced donor ability is expected for these sites.

These results show that the use of an embedding in point charges to represent the electrostatic potential of a fully ionic material produces reasonable results in terms of electronic structure of the BaO surface. In the following we will provide additional support to this conclusion based on the comparison of cluster calculations with periodic calculations reported in the literature.[7]

3.2. NO Adsorption on BaO. Recent accurate investigations have shown that NO does only physisorb on the MgO(100) surface.[4] The NO molecules form weakly bound $(NO)_2$ dimers[33] which desorb from the surface around 80 K.[34] On the low-coordinated cations of the MgO surface, the slightly larger electric field allows stabilization of isolated NO molecules.[4] The weak interaction is mainly due to electrostatic forces. Only low-coordinated anion sites give rise to the formation of chemisorbed NO species which are stable up to 450 K. These species however are not very abundant.[4]

On the BaO(100) surface the NO molecule binds quite strongly with the O_{5c} anions, $E_{ad} = 0.80$ eV, forming a relatively short O_{5c}−NO distance, 1.53 Å (Figure 1). Thus, NO chemisorbed at terrace sites should be thermally stable up to room temperature. The molecule is tilted from the surface normal, forming an O−N−O_{5c} angle of 109°. The partially negatively charged O atom of the NO molecule is equidistant from the two neighboring Ba cations on the surface (r(Ba−ON) = 2.92 Å). The spin is entirely localized on the NO molecule, as shown by both the spin density values and by the hyperfine isotropic coupling constants, Table 1. Almost no spin density is found on the surface oxide anion. The bonding has a covalent character with a significant charge delocalization over NO. The occurrence of a flow of charge is shown by the Mulliken charges (Table 1), but even more by the shift in the core level binding energies (BEs) of the O(1s) and N(1s) levels of the NO molecule. Going from the NO to the NO^- gas-phase molecules, both the O(1s) and the N(1s) core levels shift by about 10 eV to smaller BEs as a result of the increased Coulomb repulsion due to the extra electron in the valence. When NO is adsorbed on the BaO terrace, the shifts are large and in the same direction: −3.8 eV for N(1s) and −6.0 eV for O(1s), Table 1. At the same time, we notice a net shift of the 1s level of the O_{5c} surface atom to higher binding energies: $\Delta\epsilon = +3.0$ eV, Table 1. These results clearly indicate the occurrence of a substantial charge flow from the filled 2p levels of the O_{5c} anion to the π levels of the NO molecule.

TABLE 1: Computed Properties of the NO Molecule Bound at Various Sites of the BaO Surface[a]

	terrace, O_{5c}	step, O_{4c}	corner, O_{3c}
E_{ad}, eV	0.80	1.65	1.37
$\Delta q(O_{nc})$	+0.66	+0.79	+0.73
Δq(NO)	−0.80	−1.04	−1.02
spin(O_{nc})	0.03	0.10	0.08
spin(N)	0.63	0.67	0.70
spin(O)	0.31	0.21	0.19
$a_{iso}(O_{nc})$, G	−2.1	−6.4[b]	−4.7
a_{iso}(N), G	13.2	16.1[c]	14.9
a_{iso}(O), G	−17.1	−12.2[d]	−10.0
ν(N−O), cm^{-1}	1235		
δ(O−NO), cm^{-1}	670		
$\Delta\epsilon(O_{nc},1s)$, eV	+3.0	+2.2	+1.6
$\Delta\epsilon$(N,1s), eV	−3.8	−5.8	−5.2
$\Delta\epsilon$(O,1s), eV	−6.0	−8.3	−7.5

[a] E_{ad} = adsorption energy, corrected for the BSSE; Δq(X) = change in Mulliken charge on atom X going from the noninteracting systems to the surface complex; spin(X) = spin population on atom X; a_{iso}(X) = isotropic coupling constant for atom X; ν and δ are the stretching and bending vibrational modes; $\Delta\epsilon$ = core level binding energy shift computed with respect to the free BaO cluster and NO molecule. [b] The anisotropic dipolar part of the **A** matrix is $B_1 = 7.6$ G, $B_2 = 6.7$ G, $B_3 = -14.3$ G. [c] The anisotropic dipolar part of the **A** matrix is $B_1 = -11.0$ G, $B_2 = -10.7$ G, $B_3 = 21.7$ G. [d] The anisotropic dipolar part of the **A** matrix is $B_1 = 14.0$ G, $B_2 = 13.3$ G, $B_3 = -27.3$ G.

This donation of charge results in another observable property, the elongation of the N−O bond which goes from 1.16 Å in gas-phase NO to 1.28 Å in adsorbed NO. This elongation causes a consequent decrease in the N−O stretching frequency. The N−O stretching computed with the present exchange-correlation functional and basis set for free NO is 1883 cm^{-1} (after application of the scaling factor); the experimental value is 1876 cm^{-1}.[35] Upon adsorption, the N−O stretching shifts to 1235 cm^{-1} (Table 1), a value which is even lower than that computed for the gas-phase NO^- ion, 1389 cm^{-1}. In this respect one has to mention that it has been observed that the computed frequencies of molecules adsorbed on ionic substrates are often too low due to both limitations of the DFT approach and the presence of nonuniform electric fields generated by the surrounding point charges.[36]

To summarize, the BaO surface exhibits a strong reactivity of the regular surface sites toward NO, at variance with the MgO surface. Next we consider the low-coordinated sites at steps and corners. On polycrystalline materials these sites can represent 10% or more of the total number of exposed ions.

NO binds on an O_{4c} ion on a step, Figure 2, or on an O_{3c} ion on a corner, Figure 3, with E_{ad} values of 1.65 and 1.37 eV, respectively, Table 1. Thus, the binding is up to 2 times that found on the terrace sites, indicating a strong preference for NO to bind at low coordinated sites. No significant changes are observed in the spin distribution and in the hyperfine coupling constants compared to adsorption at terraces, Table

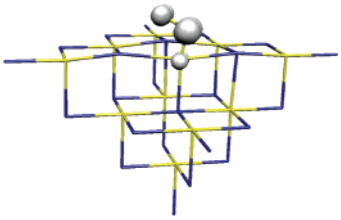

Figure 4. Spin density plot for an NO molecule adsorbed on a step site of the BaO surface.

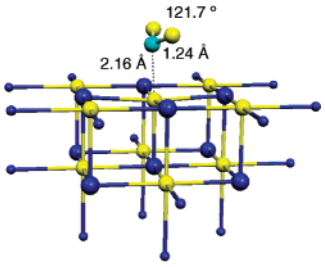

Figure 5. Optimal structure of an NO_2 molecule adsorbed N-down on an O_{5c} oxide anion at the terrace sites of the BaO surface. The surface is represented by a $Ba_9O_9Ba^*_{16}$ cluster embedded in point charges (not shown). Yellow spheres, O; sky-blue sphere, N; large blue spheres, Ba; small blue spheres, Ba*.

1: the unpaired electron is almost entirely localized on the π^* level of the NO molecule, Figure 4. The hyperfine coupling constants show that there is a nonnegligible dipolar contribution to the **A** matrix (see *B* values in Table 1), consistent with the fact that the unpaired electron is localized on the π^* orbital on the NO molecule. The strong bonding results in a short O_{nc}−NO bonding, about 1.4 Å, and in a very long N−O distance, 1.34−1.35 Å; see Figures 2 and 3. The charge transfer, as measured by the core level shifts of the N and O atoms, is even more pronounced than for the terrace case, with shifts of −5/−6 eV for the N(1s) level and of about −8 eV for the O(1s), Table 1. Correspondingly, the 1s level of the surface oxide anion shifts to larger BEs, Table 1. However, also in the case of the low-coordinated sites the bonding should be better seen as a strong covalent interaction (see, e.g., the short O_{nc}−N distance) with substantial donation to the empty NO levels.

3.3. NO_2 Adsorption on BaO. NO_2 adsorption on the (100) surface of BaO has been studied recently by plane waves periodic supercell[7,9] and cluster model[8] calculations. According to the periodic calculation of Broqvist et al.,[7] the molecule binds to an O_{5c} anion in an N-down orientation with a binding energy of 0.8 eV, a long O_{5c}−NO_2 distance of 2.39 Å, and an N−O bond length of 1.25 Å.[7] This structure is very similar to that obtained on the basis of cluster model calculations. In particular, our $Ba_9O_9Ba^*_{16}$ embedded cluster results and those obtained by Pettersson et al.[8] (see Figure 5 and Figure 1 in ref 7) agree completely. Our computed bond parameters are E_{ad} = 0.94 eV, $r(O_{5c}-NO_2)$ = 2.16 Å, r(N−O) = 1.24 Å, and α(ONO) = 122° (Figure 5). Apart from a slightly stronger bonding and shorter surface−adsorbate distance, supercell and cluster model results are quite similar. However, a recent supercell DFT calculation by Schneider finds for the same orientation of NO_2 on BaO-(100) a short O_{5c}−NO_2 distance, 1.44 Å, and a stronger bonding, 1.5 eV.[9] Schneider attributes this discrepancy to the size of the clusters or of the supercells used in the calculations,[9] but clearly more work is required to clarify this point. On the other hand, the question is not very relevant because the N-down orientation is not the most stable one, as we will discuss below.

The bonding analysis presents some interesting aspects. By reacting with the BaO surface, NO_2 forms a species that can be identified as an NO_2^- nitrite anion. This is shown by several effects. First, the population analysis shows a reduction of the negative charge on the surface oxygen and a corresponding increase on the NO_2 adsorbate. However, Mulliken charges suffer from various limitations and other measures provide better proof of the charge transfer. The most important one is the analysis of the spin density. The bond formation in fact results in an unpaired electron which is only partly localized on the NO_2 molecule and for the rest resides on the substrate; see Table 2. Since the oxide anions of the BaO surface are almost fully reduced, O^{2-},[16] the presence of a spin density on the surface oxygen indicates removal of electrons from this site. This results also in a large coupling constant of the unpaired electron with the O_{5c} nucleus of −31 G (Table 2). In principle, EPR experiments on an ^{17}O-enriched BaO sample should be able to confirm this prediction.

TABLE 2: Computed Properties of the NO_2 Molecule (N-Down, Acidic) Bound at Various Oxide Anions of the BaO Surface[a]

	terrace, O_{5c}	step, O_{4c}	corner, O_{3c}
E_{ad}, eV	0.94	1.81	1.82
$\Delta q(O_{nc})$	+0.45	+0.56	+0.64
$\Delta q(NO_2)$	−0.58	−0.88	−0.84
spin(O_{nc})	0.56	0.85	0.85
spin(N)	0.22	0.01	0.01
spin(O)	0.10	0.02	0.01
$a_{iso}(O_{nc})$, G	−31.0	−31.7[b]	−31.8
a_{iso}(N), G	42.0	3.9[c]	3.4
a_{iso}(O), G	−5.5	−0.2[d]	−0.3
ν_{asym}(N−O), cm^{-1}	1370		
ν_{sym}(N−O), cm^{-1}	1231		
δ(O−NO), cm^{-1}	734		
$\Delta\epsilon(O_{nc},1s)$, eV	+2.8	+2.6	+2.5
$\Delta\epsilon$(N,1s), eV	−3.5	−6.4	−5.4
$\Delta\epsilon$(O,1s), eV	−3.9	−6.3	−5.3

[a] E_{ad} = adsorption energy, corrected for the BSSE; Δq(X) = change in Mulliken charge on atom X going from the noninteracting systems to the surface complex; spin(X) = spin population on atom X; a_{iso}(X) = isotropic coupling constant for atom X; ν and δ are the stretching and bending vibrational modes; $\Delta\epsilon$ = core level binding energy shift computed with respect to the free BaO cluster and NO_2 molecule. [b] The anisotropic dipolar part of the **A** matrix is B_1 = 37.9 G, B_2 = 37.7 G, B_3 = −75.7 G. [c] The anisotropic dipolar part of the **A** matrix is B_1 = −0.5 G, B_2 = −0.3 G, B_3 = 0.8 G. [d] The anisotropic dipolar part of the **A** matrix is B_1 = 1.7 G, B_2 = 0.8 G, B_3 = −2.5 G.

The analysis of the core levels further shows the occurrence of the charge transfer. The N(1s) level shifts by −3.5 eV to smaller BEs; the O(1s) level of the two O atoms of the NO_2 molecule shifts by −3.9 eV. At the same time, there is a considerable stabilization of the 1s level of the O_{5c} surface anion, indicating oxidation of this atom by interaction with NO_2. The net charge transfer has important effects on the geometry of the adsorbate. The N−O bond length, which in free NO_2 is 1.21 Å, becomes 1.24 Å on the surface; also, the O−N−O bond angle changes and goes from 134° to 122°; see Figure 5. Notice that on the terrace sites the O_{5c}−N bond length, 2.16 Å, is significantly longer than in the NO case, 1.51 Å. This is due to a reduction of the covalent character of the O_{5c}−N bonding in favor of a more pronounced ionic character. Once the charge transfer has occurred, the NO_2^- fragment binds through electrostatic forces to the neighboring Ba cations and is practically detached from the surface anion where the redox process has occurred.

The structural change reflects also a shift in the vibrations. Gas-phase NO_2 has three vibrational modes at 1621 cm^{-1} (ν_{asym}), 1320 cm^{-1} (ν_{sym}), and 648 cm^{-1} (δ); the calculated values (scaled) are 1624, 1327, and 711 cm^{-1}, respectively. On the

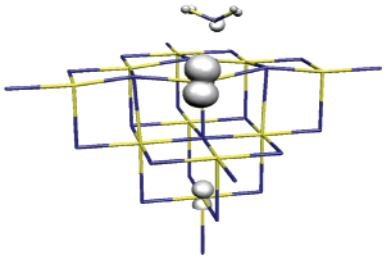

Figure 6. Spin density plot for an NO_2 molecule adsorbed on a step site of the BaO surface.

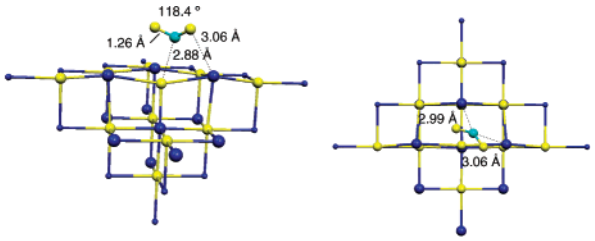

Figure 7. Optimal structure of an NO_2 molecule adsorbed N-down on an O_{4c} oxide anion at the step sites of the BaO surface (left, side view; right, top view). The surface is represented by a $Ba_{11}O_{11}Ba^*_{13}$ cluster embedded in point charges (not shown). Yellow spheres, O; sky-blue sphere, N; large blue spheres, Ba; small blue spheres, Ba*.

terrace sites, we compute the corresponding modes at 1370 cm^{-1} (ν_{asym}), 1231 cm^{-1} (ν_{sym}), and 734 cm^{-1} (δ), with significant red shifts. These modes can be compared with those computed for the gas-phase NO_2^- anion, 1281 cm^{-1} (ν_{sym}), 1261 cm^{-1} (ν_{asym}), and 748 cm^{-1} (δ).

The conclusions about the bonding nature of the NO_2 molecule are fully consistent with those reported by Broqvist et al.,[7] who also found a partial delocalization of the spin density and the formation of an ionic interaction between the adsorbate and the substrate. In the following we show that this is even more pronounced for steps and corners, a fact that cannot be neglected in the analysis of the surface reactivity.

Steps and corners exhibit an enhanced reactivity toward NO_2. On the low-coordinated anions the bonding of the molecule is ≈1.8 eV (Table 2), i.e., much larger than on the terraces. Thus, nitrite species at steps and corners are thermally very stable. The other interesting aspect is that on these sites the charge transfer is even more pronounced than on terraces. This is shown in particular by the spin density, which is almost entirely on the O_{nc} anion with no residual spin on the NO_2 adsorbate; see Table 2 and Figure 6. The isotropic hyperfine coupling constants with the N and O atoms of the NO_2 molecule are close to zero or very small (Table 2); on the other hand, large values of both a_{iso} and B coupling constants are found for the surface oxygen at a step, consistent with a large p character of the unpaired electron. This indicates that a full electron has been donated from the surface to the adsorbate. The bonding can be classified as a net charge-transfer interaction. This has important consequences for the geometry of the adsorbate; see Figures 7 and 8. The surface−adsorbate interaction is in fact dominated by electrostatic forces. The NO_2^- unit tries to maximize its interaction with the surface cations, and is partially detached from the surface oxide anion; see Figures 7 and 8. The distance of the O_{4c} or O_{3c} anions to the adsorbate increases to 2.88 and 3.09 Å, despite the strong stabilization. The fact that the surface complex has these bonding characteristics is very important for the subsequent reactivity of the species. In fact, the loss of covalent interaction with the surface oxygen and the formation of a negatively charged NO_2^- anion may imply a relatively easy

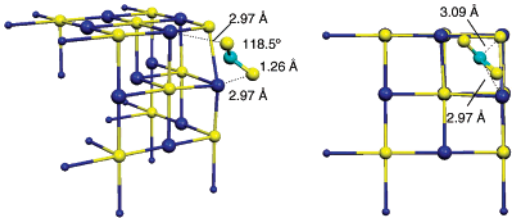

Figure 8. Optimal structure of an NO_2 molecule adsorbed N-down on an O_{3c} oxide anion at the corner sites of the BaO surface (left, side view; right, top view). The surface is represented by a $Ba_{10}O_{10}Ba^*_{12}$ cluster embedded in point charges (not shown). Yellow spheres, O; sky-blue sphere, N; large blue spheres, Ba; small blue spheres, Ba*.

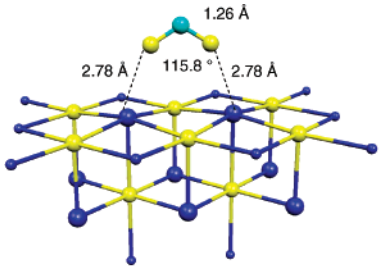

Figure 9. Optimal structure of an NO_2 molecule adsorbed O-down on a Ba_{5c} cation at the terrace sites of the BaO surface. The surface is represented by a $Ba_9O_9Ba^*_{16}$ cluster embedded in point charges (not shown). Yellow spheres, O; sky-blue sphere, N; large blue spheres, Ba; small blue spheres, Ba*.

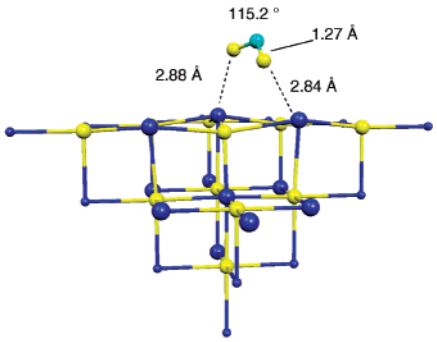

Figure 10. Optimal structure of an NO_2 molecule adsorbed O-down on a Ba_{4c} cation at the step sites of the BaO surface. The surface is represented by a $Ba_{11}O_{11}Ba^*_{13}$ cluster embedded in point charges (not shown). Yellow spheres, O; sky-blue sphere, N; large blue spheres, Ba; small blue spheres, Ba*.

diffusion of this species on the surface. Furthermore, the diffusion of the NO_2^- species leaves on the surface a very reactive O^- paramagnetic center which can be involved in subsequent reactions involving radical species.

The fact that the NO_2^- adsorbates interacts electrostatically with the surface results in a loss of directionality of the bond, and other adsorption modes are possible, such as the O-down orientation; see Figures 9−11 and Table 3. This configuration has been found also on MgO[37] and confirmed as the most stable for the sequence MgO, CaO, SrO, BaO.[8] In this orientation on the terrace sites, the two oxygen atoms of NO_2 are closer to the surface and interact with a pair of Ba cations at a distance of 2.78 Å (Figure 9). The structural changes with respect to free NO_2 are even larger than for the N-down orientation: r(N−O) = 1.26 Å and α(ONO) = 116°. This reflects a stronger interaction, E_{ad} = 1.40 eV, in agreement with the results of ref 8. The spin density is delocalized over the two nearest O_{5c} anions instead of being localized on a single oxygen as for the O-down mode. The degree of charge transfer from BaO to NO_2 is even more pronounced than for the N-down orientation. Moderate

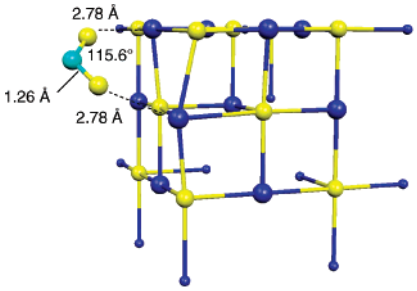

Figure 11. Optimal structure of an NO_2 molecule adsorbed O-down on Ba_{3c} cations at the corner sites of the BaO surface. The surface is represented by a $Ba_{10}O_{10}Ba^*_{12}$ cluster embedded in point charges (not shown). Yellow spheres, O; sky-blue sphere, N; large blue spheres, Ba; small blue spheres, Ba*.

TABLE 3: Computed Properties of the NO_2 Molecule (O-Down, Basic) Bound at Ba Cations on the BaO Surface[a]

	terrace, Ba_{5c}	step, Ba_{4c}	corner, Ba_{3c}
E_{ad}, eV	1.40	1.89	1.94
$\Delta q(O_{nc})$	+0.15[b]	+0.55	+0.50
$\Delta q(NO_2)$	−0.90	−0.89	−0.87
spin(O_{nc})	0.27[b]	0.84	0.87
spin(N)	0.0	0.0	0.0
spin(O)	0.0	0.0	0.0
$a_{iso}(O_{nc})$, G	−10.3	−30.9[c]	−31.9
a_{iso}(N), G	0.0	0.2[d]	0.5
a_{iso}(O), G	0.0	−0.2[e]	−0.1
ν_{asym}(N−O), cm^{-1}	1236		
ν_{sym}(N−O), cm^{-1}	1295		
δ(O−NO), cm^{-1}	749		
$\Delta\epsilon(O_{nc},1s)$, eV	+1.33[b]	+3.37	+3.60
$\Delta\epsilon$(N,1s), eV	−5.68	−5.82	−5.57
$\Delta\epsilon$(O,1s), eV	−5.61	−5.48	−5.70

[a] E_{ad} = adsorption energy, corrected for the BSSE; Δq(X) = change in Mulliken charge on atom X going from the noninteracting systems to the surface complex; spin(X) = spin population on atom X; a_{iso}(X) = isotropic coupling constant for atom X; ν and δ are the stretching and bending vibrational modes; $\Delta\epsilon$ = core level binding energy shift computed with respect to the free BaO cluster and NO_2 molecule. [b] Two O_{5c}anions, identical by symmetry, are involved in the charge transfer from the surface to the molecule. [c] The anisotropic dipolar part of the **A** matrix is $B_1 = 37.7$ G, $B_2 = 37.4$ G, $B_3 = -75.1$ G. [d] The anisotropic dipolar part of the **A** matrix is $B_1 = -0.1$ G, $B_2 = 0.0$ G, $B_3 = 0.1$ G. [e] The anisotropic dipolar part of the **A** matrix is $B_1 = 0.3$ G, $B_2 = 0.2$ G, $B_3 = -0.5$ G.

isotropic and large anisotropic coupling constants are computed for the two oxygen anions closest to NO_2, a sign of spin localization in 2p orbitals.

Core level shifts are larger than those for the N-down orientation, except for adsorption at terraces. Here, since the charge transfer involves mainly two O_{5c} anions, the positive shift in the O(1s) level, +1.33 eV, is reduced compared to the N-down case. The elongation of the N−O bonds causes a strong red shift of the stretching frequencies: 1236 cm^{-1} (ν_{asym}) and 1290 cm^{-1} (ν_{sym}). The bending mode is only slightly affected: 749 cm^{-1} (δ). These values are almost coincident with those computed for the free NO_2^- species. Experimentally, bands at ≈1215, ≈1290−1310, ≈1400, and ≈1540 cm^{-1} have been measured in IR spectra.[38,39] It is tempting to assign the bands observed at 1215 and 1290−1315 cm^{-1} to the species described above, but the poor resolution of the IR spectra and the presence of other species on the surface make this assignment purely tentative.

The interaction energy for for the O-down orientation is in general larger than that for the N-down mode. This is quite evident for the terrace sites, where the adsorption energy is 1.4 eV instead of 0.9 eV. On the steps and corners, however, the energy difference between the two orientations is too small (0.1 eV) to draw firm conclusions about the preferred adsorption mode. On the step and corner sites the NO_2 molecule lies 2.8−2.9 Å above the Ba cations, (Figures 10 and 11). r(N−O) and α(ONO) are similar to those for the N-down mode. Also, the charge transfer and spin density distribution are identical and characteristic of a nitrite species. The hyperfine coupling constants computed for the NO_2 adsorbate are almost zero, indicating complete electron transfer from the surface.

We conclude that while on terraces O-down NO_2 is favored and presents a higher degree of charge transfer with respect to the N-down orientation, on low-coordinated sites the two adsorption modes are equally stable and characterized by a complete electron transfer leading to formation of true nitrite species, electrostatically adsorbed on the surface.

4. Conclusions

The high reactivity of the BaO surface toward nitrogen oxides is a direct consequence of the electronic structure of the material. The surface basicity of the alkaline-earth oxides increases going from MgO to BaO. This change, which in the past has been rationalized in terms of different charges of the oxide anions, is easily explained in terms of the change in the Madelung potential.[13] The O^{2-} anion is unstable in the gas phase, where it dissociates into $O^- + e^-$, but becomes stable in ionic oxides because of the effect of the Madelung potential. A strong Madelung potential leads to a stable, less basic, O^{2-} species; a weak Madelung potential leads to an unstable, more basic, O^{2-} anion. On the oxides with NaCl-type structure the Madelung potential is largest in the bulk, slightly reduced on the (100) terraces, and decreases considerably on low-coordinated anions.[40] In this way it is possible to explain also the different reactivity (basicity) of oxide anions located in different positions of the surface. When one compares the same sites, e.g., terraces, on different oxides, e.g., MgO and BaO, the change in the Madelung potential is given by the longer cation−anion distance (assuming no variations in the ionic charges). This means that the Madelung field is much lower on the terrace sites of BaO than on those of MgO. The direct consequence is that the top of the O(2p) valence band (donor levels) on MgO is at lower energy (more stable) than in BaO, and that completely different reactivities can be expected.

This is indeed the case for the interaction of NO and NO_2 molecules with the two oxides. On MgO virtually no reactivity is observed, except for some minority species forming at a few low-coordinated sites (corners, kinks, etc.).[4] BaO, on the contrary, shows a strong reactivity already on the terrace sites, where both NO and NO_2 form very stable surface complexes. The fact that the (100) flat terraces are so reactive, however, does not mean that extended or point defects have no role in the surface reactivity. In this study we have shown that oxide anions at steps and corners exhibit the tendency to interact much more strongly with the adsorbed molecules, a fact that can have important consequences for the global reactivity of the surface.

While NO is bound covalently to the surface (but the bonding has a substantial polar character due to the flow of charge from BaO to the adsorbed molecule), NO_2 oxidizes the surface and forms a stable NO_2^- diamagnetic species which interacts electrostatically with the surface cations. This leaves on the surface paramagnetic O^- ions incorporated in the lattice of the BaO surface. These centers are very reactive (e.g., they are believed to be the species which promote the methane coupling reaction).[41] The charge-transfer process is more effective on low-

coordinated sites such as steps and corners but occurs also on the terrace sites. In this respect the reaction with NO_2 leads to an activation of the surface with creation of new reactive centers.

Acknowledgment. This work has been supported by the Italian INFM through the initiative of "Calcolo Parallelo" and by the Italian MIUR through a Cofin project. M.M.B. thanks the Italian and Argentinian Foreign Ministries for financial support given in the framework of an Italian−Argentinian program of scientific exchange. We thank Annalisa Del Vitto and Alessandro Figini for their suggestions and discussions.

References and Notes

(1) Amberntsson, A.; Persson, H.; Engstrom, P.; Kasemo, B. *Appl. Catal. B* **2001**, *31*, 27.
(2) Laurent, F.; Pope, C. J.; Mahzoul, H.; Del fosse, L.; Gilot, P. *Chem. Eng. News* **2003**, *58*, 1793.
(3) Schneider, W. F.; Hass, K. C.; Miletic, M.; Gland, J. L. *J. Phys. Chem. B* **2002**, *106*, 7405.
(4) Di Valentin, C.; Pacchioni, G.; Chiesa, M.; Giamello, E.; Abbet, S.; Heiz, U. *J. Phys. Chem. B* **2002**, *106*, 1637.
(5) Karlsen, E. J.; Nygren, M. A.; Pettersson, L. G. M. *J. Phys. Chem. A* **2002**, *106*, 7868.
(6) Karlsen, E. J.; Pettersson, L. G. M. *J. Phys. Chem. B* **2002**, *106*, 5719.
(7) Broqvist, P.; Panas, I.; Fridell, E.; Persson, H. *J. Phys. Chem. B* **2002**, *106*, 137.
(8) Karlsen, E. J.; Nygren, M. A.; Pettersson, L. G. M. *J. Phys. Chem. B* **2003**, *107*, 7795.
(9) Schneider, W. F. *J. Phys. Chem. B* **2004**, *108*, 273.
(10) Pacchioni, G. In *The Chemical Physics of Solid Surfaces−Oxide Surfaces*; Woodruff, P., Ed.; Elsevier: Amsterdam, 2000; Vol. 9, pp 94−135.
(11) Tanabe, K.; Saito, K. *J. Catal.* **1974**, *35*, 247.
(12) Hattori, H.; Maruyama, K.; Tanabe, K. *J. Catal.* **1976**, *44*, 50.
(13) Pacchioni, G.; Ricart, J. M.; Illas, F. *J. Am. Chem. Soc.* **1994**, *116*, 10152.
(14) Becke, A. D. *J. Chem. Phys.* **1993**, *98*, 5648.
(15) Lee, C.; Yang, W.; Parr, R. G. *Phys. Rev. B* **1988**, *37*, 785.
(16) Pacchioni, G.; Sousa, C.; Illas, F.; Bagus, P. S.; Parmigiani, F. *Phys. Rev. B* **1993**, *48*, 11573.
(17) Nygren, M. A.; Petterson, L. G.; Barandiaran, Z.; Seijo, L. *J. Chem. Phys.* **1994**, *100*, 2010.
(18) Mejias, J. A.; Marquez, A. M.; Fernandez Sanz, J.; Fernandez-Garcia, M.; Ricart, J. M.; Sousa, C.; Illas, F. *Surf. Sci.* **1995**, *327*, 59.
(19) Wadt, W. R. Hay, P. J. *J. Chem. Phys.* **1985**, *82*, 284.
(20) Ferrari, A. M.; Soave, R.; D'Ercole, A.; Pisani, C.; Giamello, E.; Pacchioni, G. *Surf. Sci.* **2001**, *479*, 83.
(21) Hay, P. J.; Wadt, W. R. *J. Chem. Phys.* **1985**, *82*, 299.
(22) Frisch, M. J.; et al. *Gaussian98*; Gaussian Inc.: Pittsburgh, PA, 1998.
(23) Notice that the contraction scheme implemented in the Gaussian98 code for the Ba basis sets differs from the original one reported in ref 21.
(24) Wertheim, G. K. *J. Electron Spectrosc. Relat. Phenom.* **1984**, *34*, 309.
(25) Boys, S. F.; Bernardi, F. *Mol. Phys.* **1970**, *19*, 553.
(26) Bagus, P. S.; Pacchioni, G. *Phys. Rev. B* **1993**, *48*, 15262.
(27) Lizzit, S.; Baraldi, A.; Grosso, A.; Reuter, K.; Ganduglia-Pirovano, M. V.; Stampfl, C.; Scheffler, M.; Stichler, M.; Keller, C.; Wurth, W.; Menzel, D. *Phys. Rev. B* **2001**, *64*, 205419.
(28) Bagus, P. S.; Illas, F.; Pacchioni G.; Parmigiani, F. *J. Electron Spectrosc. Relat. Phenom.* **1999**, *100*, 215.
(29) Weil, J. A.; Bolton, J. R.; Wertz, J. E. *Electron Paramagnetic Resonance*; John Wiley & Sons: New York, 1994.
(30) Duffy, J. A. *J. Solid State Chem.* **1986**, *62*, 145.
(31) Torrance, J. B.; Lacorre, P.; Asavaroengchai, C.; Metzger, R. M. *Physica C* **1991**, *182*, 351.
(32) Sushko, P. V.; Shluger, A. L.; Catlow, C. R. A. *Surf. Sci.* **2000**, *450*, 153.
(33) Escalona-Platero, E.; Spoto, G.; Zecchina, A. *J. Chem. Soc., Faraday Trans. 1* **1985**, *81*, 1283.
(34) Wichtendahl, R.; Rodriguez-Rodrigo, R.; Härtel, U.; Kuhlenbeck, H.; Freund, H. J. *Surf. Sci.* **1999**, *90*, 423.
(35) Huber, K. P.; Herzberg, G. *Molecular Spectra and Molecular Structure, II Infrared and Raman Spectra*; Van Nostrand Reinhold: New York, 1945.
(36) Pelmenshikov, A. G.; Morosi, G.; Gamba, A.; Coluccia, A. *J. Phys. Chem.* **1995**, *99*, 15018.
(37) Miletic, M.; Gland, J.; Hass, K. C.; Schneider, W. F. *J. Phys. Chem. B* **2003**, *107*, 157.
(38) Fridell, E.; Skoglundh, M.; Westerberg, B.; Johansson, S.; Smedler, G. *J. Catal.* **1999**, *183*, 196.
(39) Fridell, E.; Westerberg, B. *J. Mol. Catal. A* **2001**, *165*, 249.
(40) Sauer, J.; Ugliengo, P.; Garrone, E.; Saunders, V. R. *Chem. Rev.* **1994**, *94*, 2095.
(41) Lunsford, J. H. *Catal. Today* **1990**, *6*, 235.